15th Triennial World Congress, Barcelona, Spain

ADAPTIVE TORQUE PULSATION COMPENSATION FOR A HIGH-TORQUE DC BRUSHLESS PERMANENT MAGNET MOTOR

Alex Seguritan * **and Max Rotunno** *

* *University of California, San Diego*
Dept. of Mechanical and Aerospace Engineering
9500 Gilman Drive
La Jolla, CA 92093-0411, U.S.A

Abstract: Brushless permanent magnet (PM) servomotors are appealing candidates for many high-performance applications. A persistent problem with PM motors is the non-uniformity in the developed torque which gives rise to a torque pulsation that varies as a function of operating conditions. In this paper an adaptive torque pulsation compensation scheme is developed. The adaptive scheme is based on a simple lumped parameter model for the motor and on the prescribed and actual angular position measurements. The compensating signal is directly added to the motor's position control signal, so that no new hardware is necessary. The adaptive scheme is implemented on a PC computer and the effectiveness of the adaptive torque pulsation compensation is demonstrated by experiments.

Keywords: Mechatronics, Motor Control, Adaptive Control, Least-Squares Estimation

1. INTRODUCTION

Electric motors are essential elements in a variety of industrial and domestic products. More specifically brushless permanent magnet (PM) servomotors are appealing candidates for many high-performance applications. In general, the use of brushless motors improves motion control in variable speed operations, and the absence of electromechanical commutation limits wear and extends the life of the motor. Brushless motors however, require an external power converter (servo amplifier) to derive the necessary commutation. In addition, velocity or position feedback control is often employed to increase the servomechanism's dynamic response and accuracy. Typical applications for imbedded PM servomotors include high-quality machine tools, high-performance positioning systems, robotics and the automotive industry. A persistent problem with PM motors is the non-uniformity in the developed torque which give rise to torque pulsation. The magnitude and frequency of the generated torque pulsation varies as a function of operating conditions such as temperature, angular velocity and angular position. Pulsating torque is defined as the sum of cogging and ripple torque (Jahns and Soong, 1996). Cogging torque is mainly attributed to interactions between the rotor magnetic flux and stator magnetic reluctance in the absence of electrical excitation. In contrast, ripple torque is generated by imperfections in the power converter and/or deficiencies in the PM motor geometry/construction that causes variability in the flux density distribution and reluctance around the airgap. As a consequence, undesired torque pulsations are generated that become inherent in PM servomotor applications. In addition to causing speed oscillations that dramatically limit the performance in high-precision feedback applications, torque pulsation can degrade servomechanism performance by exciting the mechanical resonance modes of loads coupled to the motor.

A wide variety of methods have been proposed for minimizing the disturbing torque pulsation. The methods fall into two broad categories. The first involves a comprehensive analysis of the fundamental mechanisms for torque pulsation generation and adjusting the motor design parameters to minimize them. This method tends to be effective, although may not be feasible due to:

- The inherent tradeoff between obtaining maximum average torque and minimum pulsating torque.
- The resulting motor design parameter requirements may be impractical to fabricate.
- Sensitivity to manufacturing tolerances and the high-costs incurred in requiring high accuracy assembly, magnetic material, and electronics.

The second category involves control-based schemes that actively modify the phase current excitation in order to compensate for any non-ideal characteristics in the PM motor or associated power converter. Among these schemes is the work in (Holtz and Springob, 1996) which implements a self-commissioning control scheme that identifies several motor parameters and adaptively controls the current using a microcontroller. Other methods involve minimization of torque ripple harmonics up to a suitable predetermined order by inversion through the current profile or obtaining a suitable current profile from a constrained optimization problem given known back electromotive force (EMF) profiles.

This paper presents an adaptive compensation scheme for the minimization of torque disturbances generated in a typical 3-phase industrial brushless PM servomotor. A servomotor that yields high average output torque at low speeds was specifically chosen, since in this case torque pulsations are most evident.

A parametric model for the torque pulsation disturbance is derived based on experimental observations of angular position. The parametric model captures all the sources that contribute to torque pulsation (cogging and ripple torques). It avoids the complexity of identifying each of the contributions in torque pulsation resulting from imperfections in the back-EMF profiles, offsets and undesired harmonics in each of the phase currents.

A simple on-line estimation scheme is presented to identify the principle components of the pulsating torque using the parametric model. The adaptive compensation scheme is performed under closed-loop control, and requires minimal knowledge of motor parameters, specifically the motor torque constant and time constant. The motor parameters are readily available either from the motor's specification data and/or through off-line identification experiments (Ljung, 1998), and in any case required for proper design of a feedback controller. The torque pulsation compensation scheme developed utilizes the parametric model and takes advantage of the feedback controller designed, to enhance the sensitivity and robustness already achieved by the closed-loop system. The compensation scheme is validated through on-line closed-loop experiments at slow constant velocities.

An outline for the remaining parts of this paper are as follows. First, in Section 2 a description of the experimental setup on which the experiments were conducted is given. Section 3 gives an explanation of how torque pulsation occurs and actual measurements showing the effects. Section 4 gives the necessary theory behind the proposed adaptive compensation scheme, which is then applied in Section 5 to the the experimental setup discussed in Section 2. Finally Section 6 summarizes the conclusions of this paper.

2. EXPERIMENTAL SETUP

Experimental validation of the proposed torque pulsation on-line estimation and compensation scheme was carried out using a Compumotor Dynaserv DM1030B brushless motor, that utilizes an integrated optical encoder and PWM amplifier to provide the necessary phase current commutation. The servomotor can generate a maximum torque of $30Nm$, and the PWM switching frequency is $10kHz$. The servomotor dynamics are treated as a lumped parameter model as shown in Figure 1., and justified by the fact that the motor was operated using slow angular velocities so that the generated torque pulsation harmonics and mechanical motor dynamics are an order of magnitude less than the bandwidth of the control signals. The

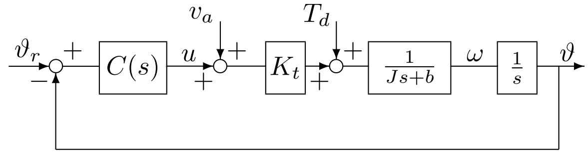

Fig. 1. DC Motor block diagram

unknown servomotor parameters K_t, J and b in Figure 1, are the motor torque constant, rotor inertia and the motor damping respectively. These parameters were experimentally determined using open-loop frequency identification techniques (Ljung, 1998). Additionally, the introduction of disturbing torque T_d and injection of compensation signal v_a with respect to the closed loop system, are shown for completeness.

The position feedback controller $C(s)$ is implemented on a PC computer using Matlab Simulink and Real-Time Workshop. The computer itself communicates with the servomotor by means of a Quansar digital signal processing system with integrated encoder inputs. The adaptive compensation scheme, to be discussed in Section 4, is also implemented on the same PC computer.

3. TORQUE PULSATION

Under ideal conditions, the torque produced by a PM motor is independent of angular position ϑ for a given excitation. The design of the DM1030B is different from the typical brushless PM motor, in that the DM1030B was designed for high torque at low speeds. In order to achieve these requirements the DM1030B is an outer-rotor servomotor that provides motion via the outside housing. The tangential electromagnetic forces generated between the rotor and stator can therefore act at a greater radius resulting in increased torque. By keeping the outer-rotor radius large, greater rotor inertia can be realized so that the motor can actuate on larger inertial loads.

Additionally, the rotor has $N_r = 124$ teeth and the stator has $N_s = 120$ teeth (12 poles with 10 teeth/pole). The large number of teeth contributes to increasing the magnetic flux density, which facilitates in torque production. The DM1030B was manufactured with this particular design so as to also increase the number of equilibrium positions provided when rotor and stator teeth align, resulting in higher rotational accuracy. Unfortunately, even with the large number of close equilibrium positions, at slow speeds the cogging torque is still present and becomes a significant source of disturbance. In view of the cogging torque being typically a phenomenon associated with generated magnetic flux seeking a minimum reluctance path, cogging torque in the DM1030B will depend on the rotor-stator relative position. Since there are an unequal number of teeth, there will be two components of cogging torque generated, one associated with the rotor teeth aligning with the stator teeth and the other from the stator teeth aligning with the rotor teeth. The number of teeth and angular frequency of rotation ω determine two cogging torque harmonics with nearly equal frequencies which are multiples of the fundamental frequencies $f_s = N_s\omega/2\pi$ and $f_r = N_r\omega/2\pi$, where the subscript s and r refer to the stator and rotor respectively and ω is the motor angular velocity in rad/sec. In addition to cogging torque, several constructive imperfections of the motor and servo drive contribute to ripple torque; the sum of these two contributions generate the resultant torque pulsation.

In the absence of torque pulsations, the expected angular velocity should be constant for a ramp reference input ϑ_r. The actual measured angular velocity of the DM1030B motor under closed loop control using a ramp input with slope $\pi/4$ is shown in Figure 2, where the effect of the torque pulsation on angular velocity is apparent. From

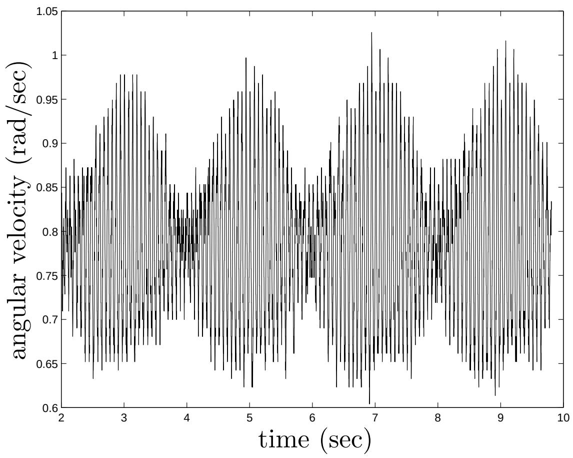

Fig. 2. Effect of torque pulsation on the motor angular velocity

the angular velocity profile seen in Figure 2 it is evident that the velocity oscillations are nearly identical to the phenomenon known as beating; i.e. the superposition of two sinusoids of nearly equal frequencies. This is in fact confirmed by the Fourier transform of the velocity profile, as shown in Figure 3, where it can be observed that the

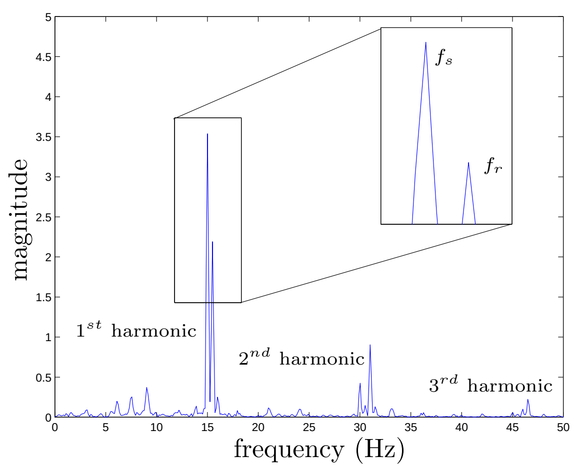

Fig. 3. Fourier transform of angular velocity

main contribution to the velocity oscillations are due to the beating of the fundamental harmonic composed of frequencies give by f_s and f_r. Since motor velocity is related to applied torque by a first order linear dynamical equation, the torque disturbance will therefore also be composed of sinusoids with deterministic frequencies f_s and f_r, but with unknown time-varying amplitudes and phases. The next section presents an adaptive online scheme to estimate the torque disturbance parameters.

4. ADAPTIVE COMPENSATION

As shown in the previous sections torque pulsation has the effect of modulating the velocity profile of a motor under constant velocity motion. The velocity deviations are predominantly generated by the first harmonic of the disturbing torque. This suggests that if the first harmonic can be compensated for, a majority of the disturbing torque pulsation can be eliminated, which results in eliminating a majority of the velocity oscillations as well. The method proposed in this paper to compensate for the disturbance torque consists of adding a signal v_a to the control signal u in Figure 1, so that $K_t v_a$ will produce a torque composed of the superposition of two sinusoids which have the same magnitude and opposite phase with respect to the dominant first harmonic of the torque pulsation disturbance.

The frequencies that constitute the first harmonic of the disturbance torque are given by $\omega_s = N_s\dot{\vartheta}(t)$ and $\omega_r = N_r\dot{\vartheta}(t)$ respectively. Since the angular position is a readily available quantity from the optical encoder in the DC motor, the frequencies ω_s and ω_r that compose the first harmonic can be considered known quantities. It is therefore necessary only to determine the amplitude and phase of each sinusoid that contributes to the first harmonic in order to be able to generate a signal that is 180° out of phase with respect to the disturbance. The unknown magnitudes and phases are estimated using a least-squares parameter estimator. Since the unknown parameters are a function of the instantaneous rotational velocity, the adaptive compensation scheme has the added benefit of being able to work under different operating conditions.

Let $\hat{T}_d$ be a parametric model of the torque pulsation based only on the first harmonics:

$$\hat{T}_d = A_s \sin(N_s\omega t + \varphi_s) + A_r \sin(N_r\omega t + \varphi_r) \quad (1)$$

where the amplitudes A_s and A_r, and the phases φ_s and φ_r are unknown quantities that need to be estimated, and the subscripts r and s refer to the rotor and stator components respectively. By simple manipulation $\hat{T}_d$ in (1) can be written as

$$\begin{aligned}\hat{T}_d = & A_1 \sin(N_s\dot{\vartheta}t) + A_2 \cos(N_s\dot{\vartheta}t) \\ & + A_3 \sin(N_r\dot{\vartheta}t) + A_4 \cos(N_r\dot{\vartheta}t) \quad (2)\end{aligned}$$

where

$$\begin{aligned}A_1 = A_s \sin\varphi_s,\ A_2 = A_s \cos\varphi_s \\ A_3 = A_r \sin\varphi_r,\ A_4 = A_r \sin\varphi_r\end{aligned}$$

From (2) it is clear that only the four parameters A_1, A_2, A_3 and A_4 have to be identified.

Following (Ioannu and Sun, 1996), a least-squares adaptive compensation scheme is devised. Let

$$\begin{aligned}\hat{\theta}^T &= [A_1,\ A_2,\ A_3,\ A_4] \\ \phi(t)^T &= [\sin(N_s\dot{\vartheta}t),\ \cos(N_s\dot{\vartheta}t), \\ &\quad \sin(N_r\dot{\vartheta}t),\ \cos(N_r\dot{\vartheta}t)]\end{aligned}$$

so that,

$$\hat{T}_d = \hat{\theta}^T\phi(t) \quad (3)$$

From the DC motor block diagram shown in Figure 1 it is possible to show that,

$$\vartheta = \frac{1}{s(Js+b)}T_d + \frac{K_t C(s)}{s(Js+b)}(\vartheta_r - \vartheta) \quad (4)$$

from which a filtered version of the real torque disturbance can be estimated as

$$\begin{aligned}\frac{1}{\Lambda(s)}T_d &= \frac{s(Js+b)+K_tC(s)}{\Lambda(s)}\vartheta - \frac{K_tC(s)}{\Lambda(s)}\vartheta_r \\ &= F(s)\vartheta - R(s)\vartheta_r \quad (5)\end{aligned}$$

It is essential to note that the above estimate for the real torque pulsation does not take into account the various noises coming into the system. The filter $\Lambda(s)$ in (5) is selected so as to make $F(s)$ and $R(s)$ proper transfer functions, and is generally chosen, in real applications, as a low pass filter in order to attenuate the effects of high frequency noise.

In order to determine the unknown parameters $\hat{\theta}$ an on-line parameter estimation, based on the least-squares (LS) algorithm with a forgetting factor, is considered:

$$\begin{aligned}\epsilon &= (F(s)\vartheta - R(s)\vartheta_r) - \frac{1}{\Lambda(s)}\hat{\theta}^T\phi(t) \\ \dot{\hat{\theta}} &= P\epsilon\phi \quad (6) \\ \dot{P} &= \begin{cases}\beta P - P\phi\phi^T P & \text{if } \|P(t)\| \le R_0 \\ 0 & \text{otherwise}\end{cases} \\ v_a &= \frac{1}{K_t}\hat{\theta}^T\phi(t)\end{aligned}$$

where v_a is the signal that is finally added to the control signal u so as to achieve the desired torque pulsation compensation. It can be shown that vector $\hat{\theta}$ of unknown parameters converge exponentially fast, since $\phi(t)$ is persistently exciting. The choice of a LS update scheme instead of a simpler gradient technique is motivated by the fact that the measurement signals are in general corrupted by noise, to which the LS scheme is less sensitive.

It is should be noted that the proposed adaptive compensation scheme only requires the measurement of the reference angle ϑ_r and the actual angle ϑ, which makes this procedure very attractive and simple to implement.

5. EXPERIMENTAL RESULTS

This section presents the results from the adaptive compensation scheme outlined in Section 4 using the experimental setup presented in Section 2. Two experiments were performed using different motor operating speeds, $\omega = \pi/10\,(rad/s)$ and $\omega = \pi/4\,(rad/s)$. The compensation scheme was enabled after 10 seconds for both experiments. In the results that follow, it can be observed that the measurement signals are corrupted by noise.

Figure 4 and Figure 5 show the angular velocity and the angular velocity spectrum for the case of $\omega = \pi/10(rad/s)$. In Figure 4 the first half of the data is without compensation and the second half (after 10 seconds) with compensation. The angular velocity spectrum in Figure 5 has been centered about the first harmonic so as to put in evidence the effects of the compensation. From the spectral data, it is apparent that the first harmonic is suppressed considerably, and that the observed residual oscillations in the compensated half of the data in Figure 4 are mainly due to the higher harmonics which are not being compensated for and noise.

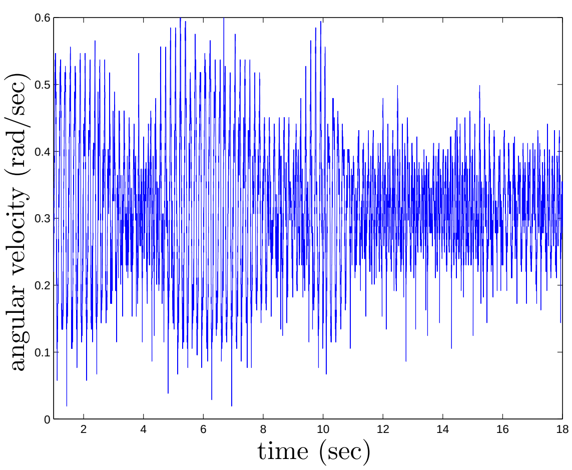

Fig. 4. Angular velocity for $\omega = \pi/10$ with compensation applied at $t = 10\,sec$

In Figure 6 and Figure 7 the angular velocity and the angular velocity spectrum for the case of $\omega = \pi/4(rad/s)$ are shown. Comparing the spectrum of the angular velocities in Figure 5 and Figure 7 it is evident that the compensation scheme is more effective and achieves greater reduction in torque pulsation disturbance when the motor speed is lower. This is attributed to that fact that at faster speeds the torque pulsation disturbance amplitude is reduce, which implies that the magnitudes of the fundamental harmonics are considerably less. In this case the identification scheme is adversely affected in regards to effectively estimating the torque disturbance parameters, from a decrease in signal-to-noise ratio (SNR). The SNR decrease is due not only

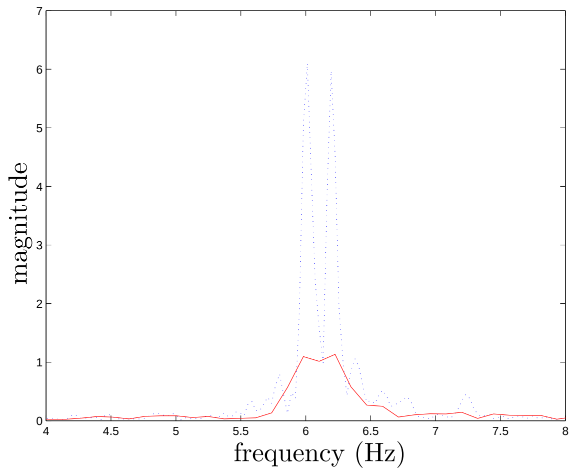

Fig. 5. Angular velocity spectrum for $\omega = \pi/10$, without compensation (dotted) and with compensation (solid)

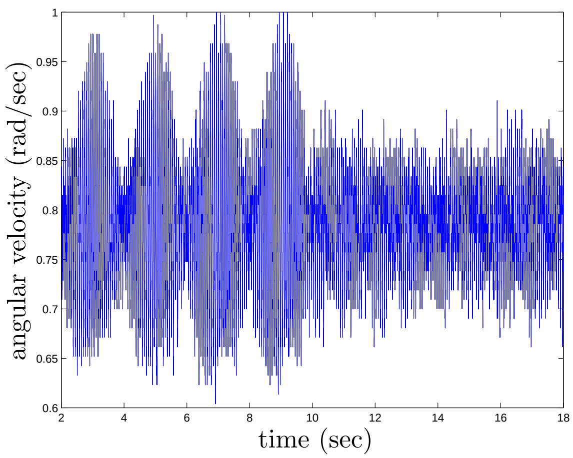

Fig. 6. Angular velocity for $\omega = \pi/4$ with compensation applied at $t = 10\,sec$

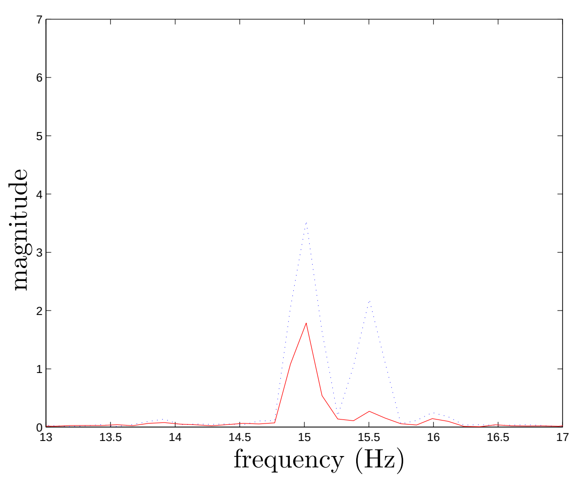

Fig. 7. Angular velocity spectrum for $\omega = \pi/4$, without compensation (dotted) and with compensation (solid)

to a reduction in magnitude of the fundamental harmonics of the torque disturbance itself, but also to the increase in noise from the resolver (position encoder) at higher motor speeds. The increase in noise can easily be seen by comparing Figure 4 and Figure 6.

6. CONCLUSIONS

This paper presents an on-line identification and compensation scheme that effectively mitigates torque pulsation in high-torque brushless PM motors. The method is extremely attractive in that the identification and compensation scheme is simple and integrates with any off the shelf commercially available servo-motor system, under closed-loop control. An estimate of torque pulsation amplitude and phase is obtained through proper filtering of system signals (output and reference), which are readily available. The compensation scheme is a consequence of proper modelling of the torque pulsation phenomenon and accounting for the torque disturbance in the closed loop system. The proposed scheme simultaneously compensates for cogging and ripple torque.

Two experiments under different operating speeds are presented to validate the proposed method. The effectiveness of the method in suppressing velocity oscillations in the motor has been demonstrated through the experiments. The method is most effective for slow speed operations due to the increase in signal to noise ratio when estimating the unknown torque disturbance parameters. The method considered is easily extendable to compensate for higher harmonics contained in the torque disturbances, which will further minimize the effect of generated torque pulsations.

ACKNOWLEDGEMENTS

This work was supported in part by the California Space Institute. The authors would also like to thank Professor Alan Schneider from UCSD, Stephen Witte of Hewlett Packard and Maurizio Pari from the University of Bologna, Italy, for the valuable discussions and insight on torque pulsation in electric motors.

REFERENCES

Holtz, J. and L. Springob (1996). Identification and compensation of torque ripple in high–precision permanent magnet motor drives. *IEEE Transactions on Industrial Electronics* **43**(2), 309–320.

Ioannu, P.A. and J. Sun (1996). *Robust Adaptive Control*. Prentice Hall.

Jahns, T.M. and W.L. Soong (1996). Pulsating torque minimization techniques for permanent magnet ac motor drives – a review. *IEEE Transactions on Industrial Electronics* **43**(2), 321–330.

Ljung, L. (1998). *System Identification*. Prentice Hall.